Journal of Membrane Science 446 (2013) 201–211

Contents lists available at SciVerse ScienceDirect

Journal of Membrane Science

journal homepage: www.elsevier.com/locate/memsci

Bacterial anti-adhesive properties of polysulfone membranes modified with polyelectrolyte multilayers

Li Tang [a], Wenyu Gu [a], Peng Yi [a], Julie L. Bitter [b], Ji Yeon Hong [a], D. Howard Fairbrother [b,c], Kai Loon Chen [a,*]

[a] Department of Geography and Environmental Engineering, Johns Hopkins University, Baltimore, MD 21218-2686, USA
[b] Department of Chemistry, Johns Hopkins University, Baltimore, MD 21218-2686, USA
[c] Department of Materials Science and Engineering, Johns Hopkins University, Baltimore, MD 21218-2686, USA

ARTICLE INFO

Article history:
Received 29 October 2012
Received in revised form
4 May 2013
Accepted 23 June 2013
Available online 1 July 2013

Keywords:
Anti-adhesive membrane
Biofouling
Poly(acrylic acid)
Poly(allylamine hydrochloride)
Polyelectrolyte multilayer

ABSTRACT

The bacterial anti-adhesive properties of polysulfone (PSU) microfiltration membranes modified with poly(allylamine hydrochloride) (PAH)/poly(acrylic acid) (PAA) polyelectrolyte multilayers (PEMs) were investigated in this study. Using a direct microscopic observation membrane filtration system, the deposition kinetics of *Escherichia coli* cells on the membrane surfaces, as well as the reversibility of bacterial deposition, were examined in the absence and presence of calcium. The PEM-modified membranes exhibited significantly improved bacterial anti-adhesive properties compared to the PSU base membranes in both the tested solution chemistries. Specifically, the bacterial deposition kinetics on the modified membranes were slower than the deposition kinetics on the base membranes. Furthermore, the bacterial removal efficiency was significantly enhanced from $<10\%$ to as high as 99% after PEM modification. Interaction force measurements conducted through atomic force microscopy revealed strong, long-ranged repulsive interactions between a carboxylate modified latex colloid probe and PEM-modified membranes, while attractive interactions were detected between the colloid probe and PSU base membranes. The bacterial anti-adhesive properties exhibited by the PEM-modified membranes were attributed to the highly swollen and hydrated PEMs that inhibit the direct contact or close approach of bacteria to the underlying PSU membranes.

1. Introduction

Low pressure membranes (LPMs) are porous membranes that can be used at relatively low transmembrane pressures (less than 200 kPa). Microfiltration (MF) and ultrafiltration (UF) membranes are examples of LPMs, and MF and UF membranes have pore sizes of ca. 0.1–1.0 μm and 0.01–0.10 μm, respectively. LPM processes have gained popularity in drinking water treatment and wastewater reuse because of their small footprint, relatively low costs, and effectiveness in removing pathogenic microorganisms and particulate matter [1].

One of the key challenges of LPM processes is biofouling, or the formation of a biofilm on the membrane surface. As LPM filtration is continuously employed to filter water and wastewater effluents, planktonic bacteria in the bulk suspension may be transported to the membrane by the convective permeate flow, and some of the bacteria may deposit on the membrane surface. The deposited bacteria then produce extracellular polymeric substances (EPS) on the membrane surface and proliferate to form microcolonies which will grow and coalesce into a biofilm. The formation of a biofilm on a LPM surface will result in higher operating pressures, poorer product water quality, frequent chemical cleaning, and shortened membrane life [2].

Among the different types of membrane fouling for LPM processes (colloidal, organic, and biological), biofouling is arguably the most serious because even a small amount of biofilm growth results in a significant loss in clean water flux [3]. Moreover, biofilms tend to be very resistant to biocides because the microorganisms are protected by the matrix of EPS. Thus, it is extremely difficult to clean membranes that have been fouled by biofilms [4]. Currently, efforts to retard biofouling have centered on the use of disinfectants (e.g., chlorine). However, disinfectants are not always successful in controlling biofouling since it is impossible to inactivate all microorganisms in the influent waters and only a small number of microorganisms are required to form a biofilm [2,4]. Furthermore, the prolonged exposure of membranes to disinfectants can damage membrane structures which will result in the decline in the membranes' ability to reject contaminants [5,6]. The use of disinfectants can also lead to the generation of potentially carcinogenic disinfection byproducts [7].

* Corresponding author. Tel.: +1 410 516 7095; fax: +1 410 516 8996.
E-mail address: kailoon.chen@jhu.edu (K.L. Chen).

0376-7388/$ - see front matter © 2013 Elsevier B.V. All rights reserved.
http://dx.doi.org/10.1016/j.memsci.2013.06.031

The initial bacterial deposition and adhesion play a critical role in the development of biofilms on membrane surfaces [8]. While the initial transport of planktonic bacteria to a membrane surface is mainly controlled by hydrodynamic factors (such as cross-flow velocity and permeate flow rate), the initial adhesion of bacteria on the membrane surface is governed by both hydrodynamic factors and interfacial interactions between the bacteria and membrane. It is generally understood that bacteria–membrane interfacial interactions can be comprised of electric double layer, van der Waals, steric (or electrosteric), and hydrophobic interactions. Past studies have demonstrated that membranes that are highly negatively charged or hydrophilic tend to exhibit strong bacterial anti-adhesive properties [2,9,10].

Several techniques have been explored, in recent years, to modify membrane surfaces with the goal of developing anti-biofouling membranes. One of the emerging techniques is the modification of membranes with polyelectrolyte multilayers (PEMs). PEMs can be assembled on a substratum through the layer-by-layer (LbL) adsorption technique [11–13]. This technique involves exposing the substratum, e.g., a membrane, to oppositely charged polyelectrolytes in a sequential manner, thus resulting in the electrostatic-driven adsorption of polyelectrolyte films on the substratum through the overcompensation of surface charge with the adsorption of each polyelectrolyte layer [14]. The main advantage of PEM modification is that it allows for the convenient construction of surface coatings with nanoscale control over the film thickness, composition, and surface chemistry [15]. In addition, PEM modification has been used to inhibit the attachment of cells on material surfaces [15,16]. For instance, Mendelsohn et al. [16] assembled highly hydrated PEM films comprised of poly (allylamine hydrochloride) (PAH) and poly(acrylic acid) (PAA) on polystyrene substrata that were remarkably resistant to the adhesion of an extremely adhesive murine fibroblast cell line.

While the modification of membranes with PEMs has been found to enhance the selectivity of ion rejection [17–21], only a few studies, to date, have reported the application of PEM modification to enhance membranes' resistance to fouling. Shan et al. [22] reported the reduction in fouling by silica colloids when polyethersulfone (PES) membranes were modified with PEMs comprised of PAH and poly(styrene sulfonate) (PSS). Wang et al. [20] demonstrated in their study that the modification of polyacrylonitrile (PAN) membranes with PEMs comprising fewer than 5 bilayers of sulfonated poly(ether ether ketone) and branched polyethyleneimine can retard organic fouling by bovine serum albumin, sodium alginate, and humic acid due to the hydrophilic nature of the PEMs. Diagne et al. [23] assembled 1.5 bilayers of PSS and poly(diallyldimethylammonium chloride) (PDADMA) on PES membranes, and they observed that the PSS/PDADMA multilayer-modified membranes were more resistant to fouling by humic acid, as well as the adhesion of *Escherichia coli* cells, compared to unmodified membranes. The authors attributed the anti-fouling properties of the PEM-modified membranes to the enhancement of surface charge and hydrophilicity of the modified membranes. Qi et al. [24] showed that the assembly of 3 PAH/PSS bilayers on the feed-solution side of a PAN forward osmosis membrane can enhance its resistance to fouling by dextran and alginate. In addition, PEMs have been used to incorporate biocidal agents, e.g., silver nanoparticles, on the membrane surfaces to inactivate deposited bacteria [23,25].

The objective of this research is to examine the bacterial anti-adhesive properties of polysulfone (PSU) MF membranes that are modified with PEMs comprised of PAH and PAA. In this study, PSU base membranes are modified with PAH/PAA PEMs using the LbL adsorption technique with the employment of a flow cell. A direct microscopic observation membrane filtration system is used to observe the deposition of fluorescent *E. coli* cells on PEM-modified membranes under a constant permeate flux and a constant cross-flow velocity in the absence and presence of calcium cations (10 mM NaCl and 1 mM $CaCl_2$+7 mM NaCl, respectively). After the deposition stage of each filtration experiment, the reversibility of bacterial deposition on the PEM-modified membrane is evaluated by first rinsing the membrane with the same solution that is used for bacterial deposition, followed by a low-ionic strength solution (1 mM NaCl), in the absence of permeate flux. The deposition kinetics and reversibility of bacterial deposition for the PEM-modified membranes are then compared to the values for the PSU base membranes in order to assess the anti-adhesive properties of the modified membranes. Our results show that the modification of PSU membranes with PAH/PAA PEMs can reduce the bacterial deposition kinetics and significantly enhance the reversibility of bacterial deposition both in the absence and presence of calcium. Interaction forces between a carboxylate modified latex (CML) colloid probe and the membrane surfaces are measured through atomic force microscopy (AFM) to elucidate the mechanisms for the bacterial anti-adhesive properties of the PEM-modified membranes.

2. Materials and methods

2.1. Base membranes

In this study, PSU membranes (Pall Corporation, Ann Arbor, MI) were used as the base membranes on which PEMs were assembled. The MF membranes are asymmetric in structure and have a nominal pore size of 0.2 μm on the active side. Through attenuated total reflection infrared spectroscopy (ATR-IR) analysis, the composition of the membranes was verified to be PSU. Details about the ATR-IR analysis are provided in the Supporting Information (SI) and the ATR spectrum is presented in Fig. S1 of the SI. The membranes were received as flat sheets and cut into smaller coupons. The membrane coupons were then rinsed and soaked in deionized (DI) water (Millipore, Billerica, MA) for at least three days at 4 °C before use.

2.2. Polyelectrolytes

PAH (M_w=15,000) and PAA (M_w=50,000) were purchased from Sigma-Aldrich (St. Louis, MO) and Polysciences, Inc. (Warrington, PA), respectively. Both polyelectrolytes were used as received without any further purification. The PAH and PAA solutions that were used to modify the membrane surfaces were prepared by dissolving the polyelectrolytes in DI water and were used within eight days after preparation. The concentration of both polyelectrolyte solutions was 20 mM (based on the repeat unit molecular weight). The ionic strength of both polyelectrolyte solutions were adjusted to 150 mM with NaCl, and the pH was adjusted to 3.0 with either 1 M HCl or 1 M NaOH.

2.3. Membrane modification by layer-by-layer adsorption technique

PSU membranes were modified with PAH/PAA multilayers through the LbL adsorption technique using an approach similar to that of Mendelsohn et al. [16]. A custom-made flow cell was used for membrane modification. The flow cell comprised two polycarbonate plates, and the cross-flow channel was 89.0 mm in length, 45.0 mm in width, and 2.5 mm in height. The PSU membrane to be modified was held tightly between the top and bottom plates with double O-rings, with the active side facing the top plate, to provide a leak-proof seal. To assemble a single bilayer of PAH and PAA on the PSU membrane surface, the active side of the PSU membrane was first rinsed with a PAH solution for 12 min

using a gear pump (Cole-Parmer, Vernon Hills, IL). After that, it was flushed with a 150 mM NaCl and pH 3.0 rinse solution (with no polyelectrolytes) for 12 min to flush away the excess or loosely bound polyelectrolytes from the membrane surface. The adsorption of PAA on the membrane was then achieved by rinsing the membrane with a PAA solution before being flushed with a rinse solution. This process is then repeated $n-1$ times in order to achieve a total of n bilayers on the membrane. The cross-flow velocities used for polyelectrolyte adsorption and for flushing with a rinse solution were 0.75 mm/s and 2.25 mm/s, respectively. 1–8 PAH/PAA bilayers were assembled for X-ray photoelectron spectroscopy (XPS) analysis, while 2 bilayers were assembled for the bacterial deposition and release experiments.

Surface morphologies of the base and PEM-modified membranes were acquired using scanning electron microscopy (SEM, Quanta 200, FEI, Hillsboro, OR). The membranes for SEM analysis were vacuum-dried in a desiccator overnight and examined under the low-vacuum mode. The vacuum-dried membranes were also imaged using an atomic force microscope (AFM, Multimode NanoScope IIId, Bruker Nano Inc.) to obtain the surface topology and surface roughness. Details about the AFM imaging analysis are provided in the SI, and the surface topography is presented in Fig. S2 of the SI. The average hydraulic resistances of the base and PEM-modified membranes were determined by using a laboratory-built dead-end membrane filtration set-up to measure the permeate fluxes of DI water over a range of transmembrane pressures (TMPs) (up to ca. 160 kPa).

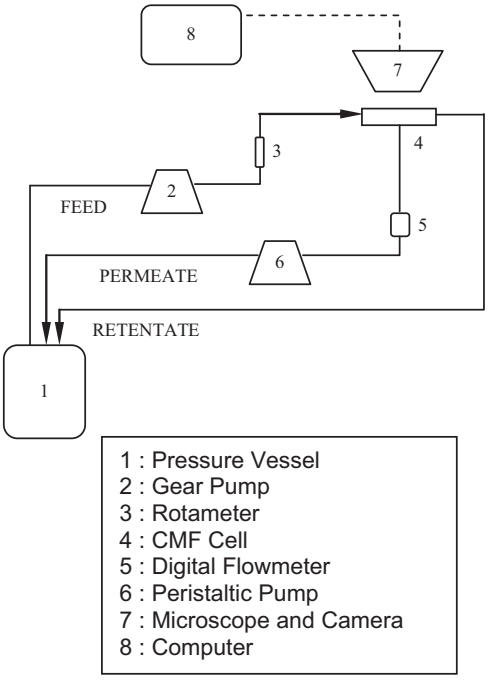

Fig. 1. Schematic of the direct microscopic observation membrane filtration system.

2.4. XPS analysis

X-ray photoelectron spectroscopy (XPS) was conducted on PSU membranes that were sequentially rinsed with PAH and PAA solutions, as described in Section 2.3, to confirm the formation of PEMs on the membrane surfaces. The XPS analysis was performed with a PHI 5400 XPS system (base pressure $< 5 \times 10^{-8}$ Torr) using Mg Kα X-rays (1253.6 eV). Samples were prepared by pressing a cut out of each membrane onto double sided copper tape (1×1 cm^2) so that no copper was visible. Photoelectrons ejected from each sample were measured with a precision high energy electron analyzer operating at constant pass-energy. Survey scans performed to determine elemental composition were completed using a pass-energy of 178.95 eV at a scan rate of 0.250 eV/step. The regions containing the desired elements of interest were analyzed at a scan rate of 0.125 eV/step using two different pass-energies: 89.45 eV for quantification purposes, and 22.36 eV to determine lineshapes and peak positions. XP spectra were processed with commercially available software (CasaXPS), and atomic concentrations were quantified by integration of the relevant photoelectron peaks.

2.5. Bacteria for membrane filtration experiments

E. coli K12 MG1655 was used as the model bacteria in this study [26]. The bacteria carry the antibiotic resistance gene and are labeled with the green fluorescent protein which allows them to be observed under a fluorescent microscope. The *E. coli* cells were incubated in a Luria Bertani broth (25 g/L, Fisher Scientific) that contained 50 mg/L kanamycin (Aldrich Chemical) at 37 °C for ca. 3 h to allow the cells to reach the exponential growth phase. The cells were then harvested through centrifugation at 4200 g for 10 min at 4 °C (Avanti centrifuge J-20 XPI, Beckman Coulter, Brea, CA), decantation of the supernatant, and re-suspension of the cell pellet in a 154 mM NaCl and pH 7.0 (buffered with 0.15 mM $NaHCO_3$) solution. The suspension was then centrifuged at 4200 g for 5 min, the supernatant was decanted, and the cell pellet was re-suspended in a 154 mM NaCl and pH 7.0 solution. This washing process was repeated once, but after the centrifugation step, the cell pellet was re-suspended in a 10 mM NaCl and pH 7.0 solution. The cell suspension was briefly vortexed before it was used to prepare the suspension for a bacterial deposition and release experiment. For all the bacterial deposition and release experiments, the cell concentration in the feed suspension was ca. 1.4×10^7 cells/L.

A ZetaPALS analyzer (Brookhaven, Holtsville, NY) was used to measure the electrophoretic mobility of *E. coli* cells at 25 °C and the zeta (ζ) potentials of the cells were calculated using the Smoluchowski equation [27]. Three cell samples were used for each solution chemistry, and 10 measurements were performed for each sample.

2.6. Direct microscopic observation membrane filtration system

The direct microscopic observation membrane filtration system used in this study was similar to the systems used in other studies [2,10,26]. The closed-loop filtration system was operated under the cross-flow mode. It comprised four main components: (1) cross-flow membrane filtration (CMF) cell, (2) pressure vessel, (3) pumping and tubing system, and (4) fluorescent microscope and digital camera. A schematic of the membrane filtration system is presented in Fig. 1. The CMF cell comprised two polycarbonate plates. A 3-mm thick glass window was inserted into the top plate to allow for the direct microscopic observation of bacterial deposition on and release from the membrane surface. The cross-flow channel inside the CMF cell was 76.0 mm in length, 25.0 mm in width, and 1.0 mm in height. The membrane to be tested was held tightly between the top and bottom plates, with the active side facing the top plate, with double O-rings to provide a leak-proof seal. A permeate spacer (McMaster-Carr, Aurora, OH) was placed below the membrane in a shallow insert of the bottom plate.

The feed bacterial suspension (volume of 2 L) was contained in a stainless steel pressure vessel (Alloy Products, Waukesha, WI) that was pressurized to ca. 170 kPa. A gear pump (Cole-Parmer, Vernon Hills, IL) was used to circulate the feed suspension through

the CMF unit at a cross-flow velocity of 10 cm/s (Re=96.2, shear rate=600.0 s^{-1}). The flow rate of the feed suspension entering the CMF unit was kept constant at 0.15 L/min, and it was monitored using a rotameter mounted on the feed line (Blue-White, Huntington Beach, CA). The permeate flux was maintained constant at 30 μm/s during the deposition experiment using an 8-roller digital peristaltic pump (Cole-Parmer, Vernon Hills, IL) mounted on the permeate line. The permeate was circulated back into the pressure vessel, and the permeate flow rate was monitored using a digital flow meter (Cole-Parmer, Vernon Hills, IL).

The CMF unit was placed on the stage of a florescent microscope (Nikon Eclipse E600W, Japan) that was equipped with a 10× objective lens. During the filtration experiment, digital images of *E. coli* cells on the membrane surface were acquired with a CCD camera (Roper Scientific, Photometrics CoolSnap ES, Germany) in real time. The deposited *E. coli* cells in the images were enumerated manually after each experiment in order to obtain the deposited cell densities as a function of time.

2.7. Direct microscopic observation of bacterial deposition and release

The bacterial deposition experiments were conducted under two different solution chemistries: (1) 10 mM NaCl and (2) 1 mM $CaCl_2$+7 mM NaCl (total ionic strength of 10 mM). The pH of all solutions was adjusted to 7.0 (buffered with 0.15 mM $NaHCO_3$). All salts used in the experiments were ACS grade (Fisher Scientific) and electrolyte stock solutions were prepared by dissolving the salts in DI water. All experiments were conducted at room temperature (23 °C).

Before each deposition experiment, the membrane was first equilibrated at a permeate flux of 30–40 μm/s for at least 40 min with the same electrolyte solution (with no bacteria) as that to be used in the deposition experiment. Just before the start of the deposition experiment, the permeate flux was adjusted to 30 μm/s. The *E. coli* cell suspension was then injected into the pressure vessel using a syringe pump (Harvard, Holliston, MA) to initiate the deposition experiment. During the deposition experiment, an image of the central part of the membrane surface was captured every 3 min. The number of deposited *E. coli* cells within the field of view of the microscope was plotted as a function of time, and the rate of increase in deposited bacteria within the field of view, k, can be obtained by determining the slope of the graph. The deposition rate coefficient of *E. coli* cells, k_{obs}, was then calculated by using the equation [2,26]:

$$k_{obs} = \frac{k}{A_m N_0} \quad (1)$$

where A_m is the area of the field of view of the microscope (between 11,900 and 150,500 μm^2) and N_0 is the number concentration of *E. coli* cells in the feed suspension (1.4×10^7 cells/L).

After each deposition experiment, a bacterial release experiment was conducted in two stages. In Stage 1, the membrane with deposited bacteria was rinsed with the same solution (with no bacteria) as that used in the deposition experiment in the absence of permeate flow. In Stage 2, the membrane was rinsed with a 1 mM NaCl solution (with no bacteria) in the absence of permeate flow. This decrease in the ionic strength of the rinse solution in Stage 2 is expected to increase the electric double layer repulsion between the bacteria and membranes and thus, to enhance the chances of bacterial release. For both release stages, the cross-flow velocity was maintained constant at 10 cm/s. At the end of each release stage, an image of the membrane was captured. The removal efficiency was calculated by normalizing the number of deposited cells remaining on the membrane after each release stage to the number of deposited cells immediately after the deposition experiment. The bacterial deposition and release experiments were carried out at least three times for each solution chemistry.

2.8. Interaction force measurements

In order to investigate the effects of PEM modification on the interactions between *E. coli* cells and membrane surfaces, the interaction forces between a CML colloid probe and membrane surfaces were measured using an AFM (Multimode NanoScope IIId, Bruker Nano Inc.) [28–32]. The CML colloid was used as a surrogate for *E. coli* cells because both CML colloids and *E. coli* cells carry carboxylic acid functional groups [26]. The CML colloid probe was prepared by attaching a CML colloid (Invitrogen, Eugene, Oregon) with a diameter of 16 μm to a 0.06 N/m tipless silicon-nitride cantilever (Bruker, Camarillo, CA) using an epoxy adhesive (Henkel Corporation, Rocky Hill, CT). Immediately before the interaction force measurements, the colloid probes were oxidized in a UV-ozone chamber (Procleaner™ 110, BioForce Nanosciences, Inc., Ames, IA) for 15 min to remove any possible organic contaminants on the probe.

All AFM force measurements between the colloid probes and membrane surfaces were conducted in a glass fluid cell. The fluid cell was rinsed with ethanol, followed by DI water, and then blow-dried with ultrapure nitrogen before and after use. The solution of interest was degassed through ultrasonication for 15 min and stored in a water bath at 27 °C before use. The solution of interest was slowly injected into the fluid cell with a syringe and force measurements were conducted by bringing the colloid probes toward the membrane surfaces and then retracting the probes upon contact. A scan rate of 0.49 Hz and ramp size of 1.0 μm were employed and the average cantilever approach and retract velocity was calculated to be 0.98 μm/s. Force–separation curves were derived from the cantilever deflection and piezo displacement obtained from the AFM measurements. For each solution chemistry, force measurements were conducted at 13–15 locations on the membrane surface and 5 measurements were taken at each location.

3. Results and discussion

3.1. Characterization of E. coli cells and PSU membranes modified with PAH/PAA multilayers

The zeta potentials of *E. coli* cells were determined to be –36.9 (±2.6) mV at 10 mM NaCl and –25.7 (±1.2) mV at 1 mM $CaCl_2$+7 mM NaCl, both at pH 7.0. The zeta potential of the *E. coli* cells in the presence of calcium was less negative than that in the absence of calcium due to the neutralization of bacterial surface charge by calcium ions [33]. In the absence of calcium, indifferent sodium ions can only screen the surface charge of *E. coli* cells.

SEM and AFM images of a PSU base membrane and a membrane modified with 2 PAH/PAA bilayers are shown in Fig. 2 and SI Fig. S2, respectively. Generally, the morphologies of the base and PEM-modified membranes looked similar, albeit some pores on the modified membrane, as observed under the SEM, seemed to be blocked by the PEM. The hydraulic resistances of the base membranes and membranes modified with 2 bilayers were 5.5×10^{10} m^{-1} and 2.3×10^{11} m^{-1}, respectively. The increase in hydraulic resistance of the membrane after PEM modification implies that the pore size of the base membrane, especially at the entrance of the pores, may be reduced when the PEM was assembled on the membrane surface. Although the hydraulic resistance of the PEM-modified membrane was about four times

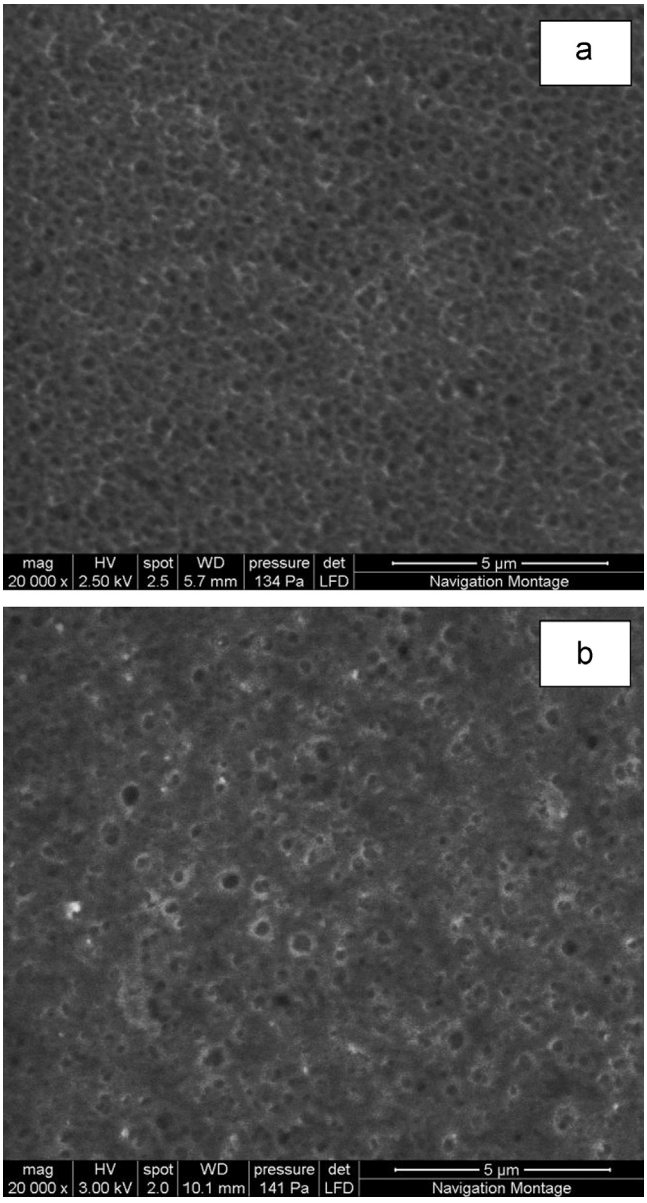

Fig. 2. SEM images of (a) a PSU base membrane and (b) a PSU membrane modified with 2 bilayers of PAH and PAA.

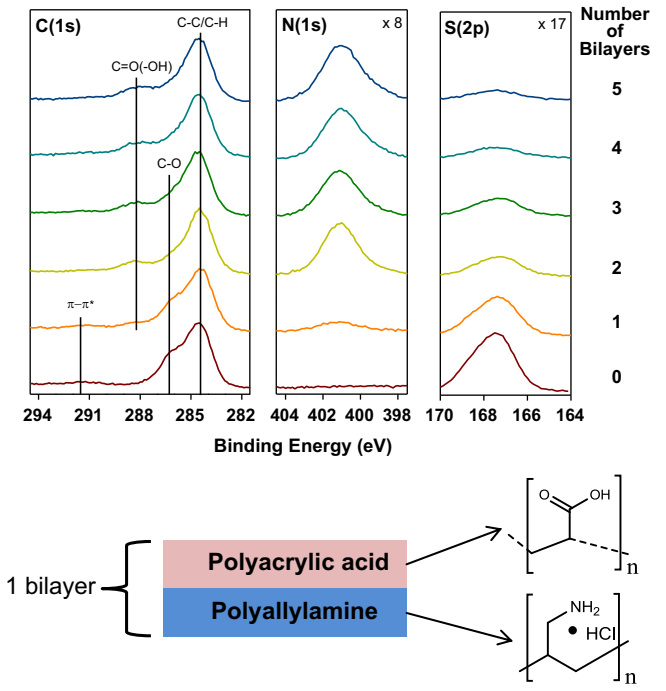

Fig. 3. Evolution of the C(1s), N(1s), and S(2p) XP spectra for a PSU membrane coated with increasing numbers of PAH/PAA bilayers. Below the XP spectra is an illustration of the structure and chemical composition of each bilayer.

of that of the base membrane, it was still within the typical range of hydraulic resistances for MF membranes.

3.2. XPS analysis of PEM-modified membranes

XPS analysis of PSU membranes with increasing numbers (1–5) of PAH/PAA bilayers added to the surface is shown in Fig. 3. As the number of bilayers increased, there was a systematic decrease in the signal intensity of the S(2p) region as the sulfone groups present in the original PSU membrane were covered by a thicker overlayer. Conversely, a signal intensity appeared in the N(1s) region at 401.2 eV due to the presence of nitrogen atoms in PAH. As the number of bilayers increased, the signal intensity in the N (1s) region steadily increased as well. The addition of the PAH/PAA bilayers also changed the C(1s) lineshape, shifting from that of a pure PSU membrane to a spectral envelope which exhibited features of the two bilayer components, PAH and PAA. These features include a noticeable and systematic decrease in C–O and π–π^* peaks as the number of PAH/PAA bilayers increased, accompanied by a steady growth of a carboxyl peak centered at 288.4 eV due to the addition of PAA. Thus, these observations demonstrate that the PEMs can be successfully assembled on PSU membranes through the LbL adsorption technique and that the composition of the PEMs on membrane surface can be controlled by varying the number of sequential exposures to the PAH and PAA solutions. Analysis of Fig. 3 also shows that after approximately 4 bilayers (membranes with up to 8 bilayers were measured), the XPS spectra remains essentially unchanged because the near surface region is now determined exclusively by the composition of the bilayers.

3.3. Influence of PEM modification on bacterial deposition kinetics

The anti-adhesive properties of the PEM-modified membranes were first tested by performing bacterial deposition experiments using the direct microscopic observation membrane filtration system at 10 mM NaCl in the absence of permeate flow. For these experiments, the permeate outlet of the CMF cell was sealed to prevent water from permeating through the membrane. The base and PEM-modified membranes were exposed to the bacterial suspensions at a cross-flow velocity of 10 cm/s for an hour, and the images of the *E. coli* cells deposited on the membranes were captured at the end of the experiments (Fig. 4a and b). The number of *E. coli* cells deposited on the PEM-modified membranes was three orders of magnitude lower than that on the base membranes (Fig. 4c). This result shows that the modification of membranes with PAH/PAA PEMs can significantly enhance their resistance to bacterial attachment when the effects of permeate drag force are absent.

In order to test the anti-adhesive properties of the PEM-modified membranes in the presence of permeate flow, deposition experiments were conducted by using the membrane filtration system at a permeate flux of 30 µm/s and cross-flow velocity of 10 cm/s. Fig. 5a and b present the number of deposited *E. coli* cells (per mm^2) on the base and PEM-modified membrane surfaces, respectively, when bacterial deposition first took place at 10 mM

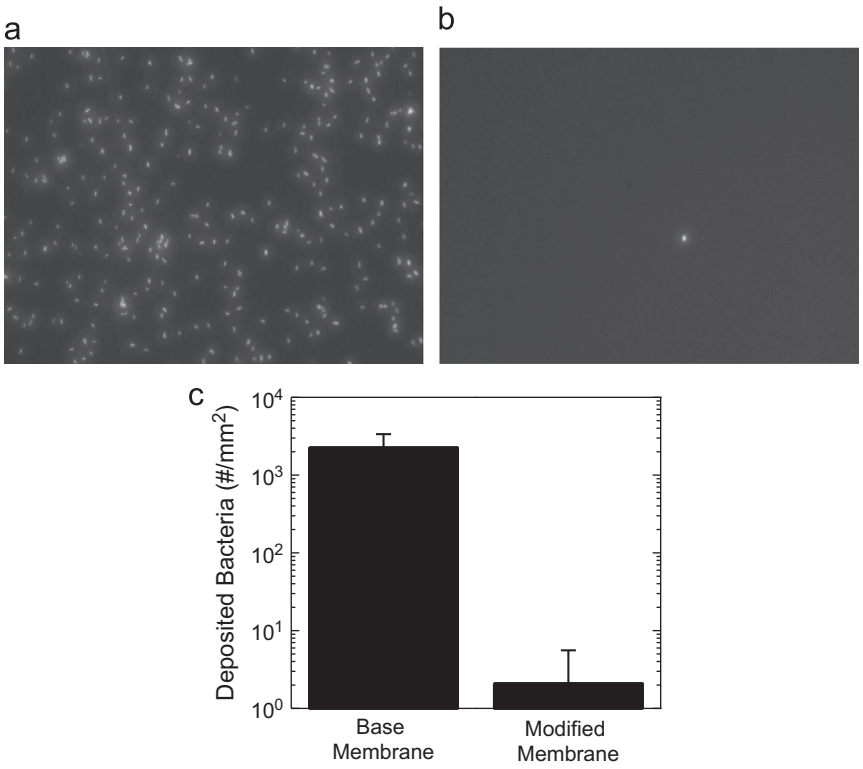

Fig. 4. Images of deposited bacteria (0.446 mm × 0.333 mm) on (a) a base membrane and (b) a PEM-modified membrane after the membrane was exposed to a bacterial suspension prepared at 10 mM NaCl and pH 7.0 for 1 h in the absence of permeate flux. (c) Number of bacteria deposited on the base and PEM-modified membranes (per mm^2). Error bars represent standard deviations.

NaCl and the membranes were subsequently rinsed with 10 mM NaCl and 1 mM NaCl solutions. For the base membrane, 5429 *E. coli* cells deposited on 1 mm^2 within a time period of 20 min. In comparison, only 2884 *E. coli* cells deposited on 1 mm^2 of the PEM-modified membrane within the same period of time. By determining the rate of increase of deposited bacteria in the deposition stage, the deposition rate coefficients, k_{obs}, were calculated using Eq. (1) and presented in Fig. 6. The average k_{obs} value for the PEM-modified membranes (17.3 μm/s) was smaller than that for the base membranes (35.8 μm/s), indicating that PEM modification was effective in enhancing the membranes' resistance to bacterial attachment even in the presence of permeate drag force.

The kinetics of bacterial deposition on membrane surfaces are known to be governed by the interfacial interactions between bacteria and membrane surfaces, as well as the drag force resulting from the permeate flow [2,26,34]. Since the permeate flux was maintained constant at 30 μm/s for both experiments conducted using the base and PEM-modified membranes, the permeate drag force exerted on the bacteria was the same for both experiments. Therefore, the lower deposition kinetics observed for the PEM-modified membranes in the deposition experiments conducted in the absence and presence of permeate flow implies that the interfacial interaction between the bacteria and membrane surfaces was more repulsive (or less adhesive) for the PEM-modified membranes compared to the base membranes at 10 mM NaCl.

In order to study the effects of calcium, deposition experiments were conducted on the base and PEM-modified membranes at 1 mM $CaCl_2$+7 mM NaCl and a permeate flux of 30 μm/s. The deposition rate coefficients obtained in the presence of calcium are presented in Fig. 6. The results show that, analogous to what was previously observed in the presence of 10 mM NaCl, the deposition kinetics of *E. coli* cells on the PEM-modified membranes (15.3 μm/s) were lower than the kinetics on base membranes (36.4 μm/s) in the presence of calcium. This result demonstrates that the modification of membranes with PAH/PAA PEMs is just as effective in reducing bacterial deposition kinetics in the presence of calcium.

3.4. Effect of PEM modification on reversibility of bacterial deposition

In addition to deposition kinetics, the reversibility of bacterial deposition can serve as a suitable gauge of a membrane's resistance to bacterial adhesion [26]. To examine the effects of membrane modification with PEMs on the reversibility of bacterial deposition, the removal efficiencies of the bacteria that were deposited at 10 mM NaCl were obtained for both the release stages. After bacterial deposition had taken place on a base membrane at 10 mM NaCl, the membrane was first rinsed with the same bacteria-free solution for 30 min, followed by a 1 mM NaCl solution for 30 min (Fig. 5a). In both release stages, hardly any release of deposited bacteria was observed. In stark contrast, when a PEM-modified membrane with bacteria that were deposited at 10 mM NaCl was rinsed with the same solution for only 10 min, 97% of the deposited bacteria were released (Fig. 5b). A subsequent rinse with a 1 mM NaCl solution for 10 min resulted in almost complete (99%) removal of deposited bacteria. Note that the time for each release stage for the PEM-modified membranes was only 10 min (compared to 30 min for base membranes) due to the fast and significant degree of bacterial release that was observed for the modified membranes. The removal efficiencies obtained from both the release stages for the base and PEM-modified membranes are shown in Fig. 7a. The significant increase in the removal efficiencies (from $< 10\%$ to close to 100%) evidently demonstrated that the modification of membrane surfaces with PEMs can dramatically enhance the reversibility of bacterial deposition in the presence of NaCl.

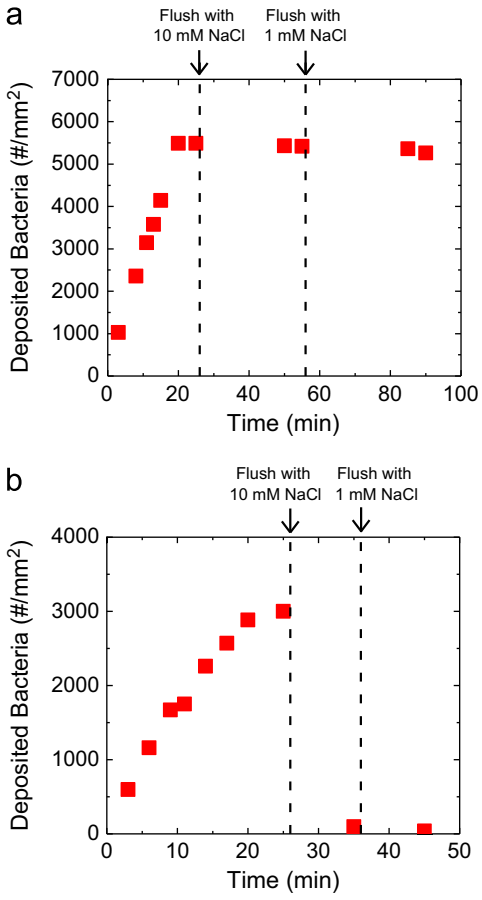

Fig. 5. Number of bacteria on (a) a PSU base membrane and (b) a PEM-modified membrane during the deposition and release stages. The deposition experiment was conducted at 10 mM NaCl and a permeate flow rate of 30 μm/s. The membrane was subsequently rinsed with a 10 mM NaCl solution, followed by a 1 mM NaCl solution, in the absence of permeate flow. For all the deposition and release stages, the pH was maintained at 7.0.

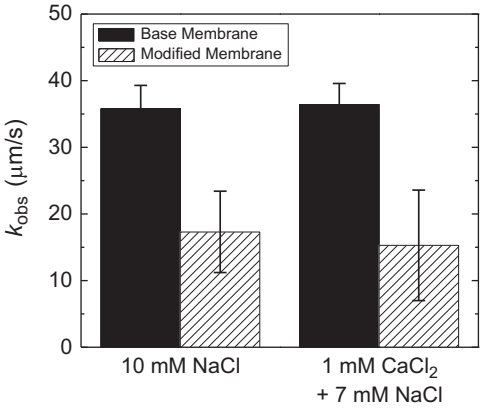

Fig. 6. Bacterial deposition rates, k_{obs}, for base and PEM-modified membranes at 10 mM NaCl and 1 mM $CaCl_2$+7 mM NaCl. The pH during the deposition process was 7.0. The permeate flow rate was 30 μm/s. Error bars represent standard deviations.

Furthermore, just before the start of the release stages (i.e., when both the cross flow and permeate flux were stopped by switching off the gear and peristaltic pumps), the *E. coli* cells deposited on PEM-modified membranes were observed under the microscope to be wriggling in their fixed positions. When the cross flow was started (with no permeate flow) to initiate the first stage

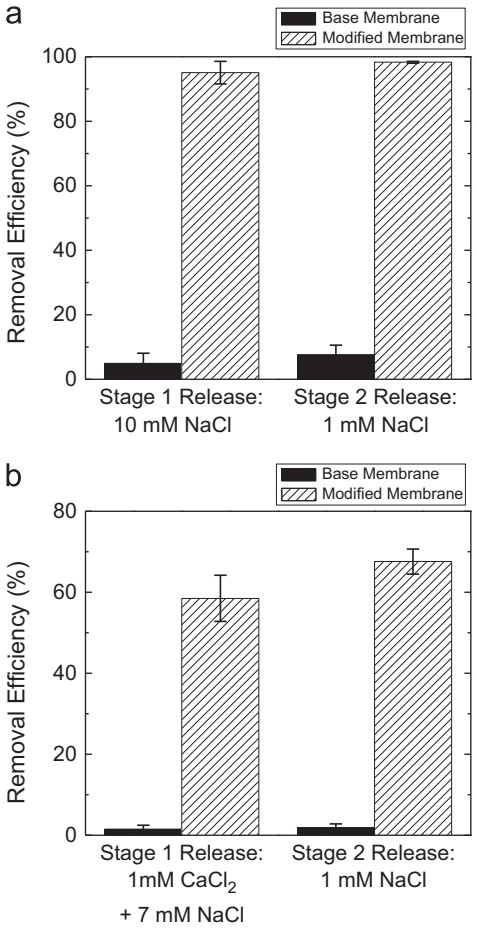

Fig. 7. Bacterial removal efficiencies for base and PEM-modified membranes after deposition at (a) 10 mM NaCl and (b) 1 mM $CaCl_2$+7 mM NaCl. The release experiments were conducted in two stages. In Stage 1, the membranes were rinsed with the same solutions that were used for bacterial deposition (either 10 mM NaCl or 1 mM $CaCl_2$+7 mM NaCl). In Stage 2, the membranes were rinsed with 1 mM NaCl solutions. The pH for both release stages was 7.0. Error bars represent standard deviations.

of the release experiment, a considerable number of the initially deposited bacteria were swept away instantly, as shown in Video 1. In contrast, the *E. coli* cells deposited on the base membranes were motionless and did not wriggle on the membrane surface in the absence of cross flow and permeate flow. Also, no bacteria were observed to be released from the base membrane surface when the cross flow was initiated. These observations suggest that the modification of the PSU membranes with PEM can substantially weaken the attachment of bacteria to the membrane surface.

The removal efficiencies obtained after the *E. coli* cells were deposited on the base and PEM-modified membranes at 1 mM $CaCl_2$+7 mM NaCl are presented in Fig. 7b. Similar to the results obtained when bacterial deposition took place on the base membranes at 10 mM NaCl, no significant release of *E. coli* cells occurred ($<3\%$) when the base membranes were rinsed with a 1 mM $CaCl_2$+7 mM NaCl solution, followed by a 1 mM NaCl solution. In the case of the PEM-modified membranes, in contrast, a substantially larger degree of release was observed when the membranes were rinsed with the two rinse solutions (59% and 68% in Stages 1 and 2, respectively). These removal efficiencies were lower than the efficiencies obtained when the bacterial deposition took place at 10 mM NaCl (97% and 99% in Stages 1 and 2, respectively). Possible reasons for the lower removal efficiencies will be discussed in the following section.

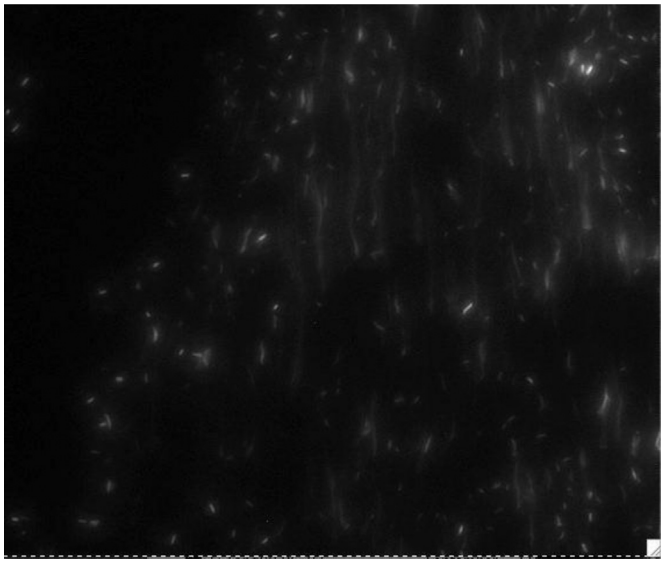

Video S1. Bacteria wriggling in their fixed positions on a PEM-modified membrane prior to the release process. A substantial number of deposited bacteria were swept away instantly when the cross flow was started. A video clip is available online. Supplementary material related to this article can be found online at http://dx.doi.org/10.1016/j.memsci.2013.06.031.

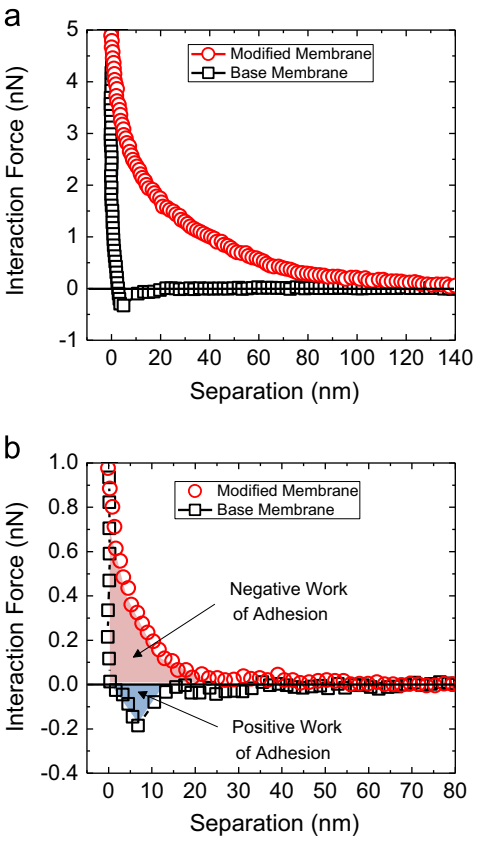

Fig. 8. Representative retract interaction force curves between a CML colloid probe and membrane surface at (a) 10 mM NaCl and (b) 1 mM $CaCl_2$+7 mM NaCl. The pH was 7.0. Positive (blue) and negative (red) work of adhesion are presented in (b). (For interpretation of the references to color in this figure legend, the reader is referred to the web version of this article.)

Nevertheless, the modification of membrane surfaces with PEMs is shown from these results to significantly enhance the reversibility of bacterial adhesion after deposition in the presence of calcium.

3.5. Proposed mechanism for anti-adhesive properties of PEM-modified membranes

Representative retraction (or pull-off) force–separation curves for the base and PEM-modified membranes obtained at 10 mM NaCl are presented in Fig. 8a. Positive and negative forces represent repulsive and attractive forces, respectively. In the case of the base membrane, the CML probe experienced a maximum adhesive force of −0.33 nN when it was retracted from the membrane surface. When the CML colloid probe was retracted from the PEM-modified membrane, in contrast, a large and long-ranged repulsive force was detected up to a separation distance of ca. 100 nm.

In order to test if the repulsion observed for the PEM-modified membrane was due to electric double layer interactions, the decay lengths for base and PEM-modified membranes, κ^{-1}, were calculated by fitting their respective approach force–separation curves obtained at 10 mM NaCl with the equation [35]:

$$F = B \exp(-\kappa h) \quad (2)$$

where F is the interaction force between the CML colloid probe and membrane surface, B is a pre-exponential constant, and h is the separation distance. The approach force–separation curves (Fig. S3 of the SI) show that repulsive forces were observed when the CML colloid probe was brought towards both membranes. The decay length for the base membrane was 3.0 nm (average of 10 measurements), which is equal to the theoretical Debye screening length at an ionic strength of 10 mM [27,36]. The identical experimental and theoretical values indicate that the interaction forces between the CML colloid probe and base membrane, both negatively charged at pH 7.0, were dominated by electric double layer interactions. In the case of the PEM-modified membrane, the approach force–separation curves overlapped with the retract force–separation curves, and the repulsive forces were markedly longer-ranged compared to the forces for the base membrane. The decay length of the PEM-modified membrane was 31.6 nm (average of 10 measurements), which was considerably longer than that of the theoretical Debye length. This discrepancy implies that another force, other than electrostatic repulsion, dominated the interactions between the CML colloid probe and PEM-modified membrane. This repulsive force is likely due to the compression of the highly hydrated and swollen PAH/PAA PEM by the CML colloid probe as the probe was brought close to the PEM-modified membrane.

In their study of the cellular anti-adhesive properties of PEMs, Mendelsohn et al. [16] demonstrated that PEMs comprising PAH and PAA will swell and become hydrated when they are first assembled under low pH conditions (pH=2.0) and then exposed to neutral pH conditions (pH=7.4). In the same work [16], the authors showed that the PAH/PAA PEMs assembled at pH 2.0 are remarkably resistant to the adhesion of a highly adhesive fibroblast cell line at pH 7.4. Lichter et al. [37] also observed that PAH/PAA PEMs assembled at pH 2.0 are mechanically soft with a relatively low elastic modulus (ca. 1 MPa) and are highly resistant to the attachment of both *E. coli* and *Staphylococcus epidermidis* bacteria at neutral pH conditions. Similar to the findings of these two groups, we showed in this study that PAH/PAA PEMs assembled on PSU membranes at pH 3.0 can inhibit the adhesion of *E. coli* cells at pH 7.0.

PAH and PAA are weak polyelectrolytes which contain amine and carboxylic acid functional groups, respectively. At a low pH of 3.0, the amines of PAH (pK_a≈9) are nearly fully protonated (NH_3^+) and thus PAH is highly positively charged. Conversely, at pH 3.0, most of the carboxylic acids of PAA (pK_a≈5) remain protonated (COOH), resulting in PAA to be only partially negatively charged. Hence, when a PEM comprising PAH and PAA layers is assembled on a PSU membrane at pH 3.0, there are relatively few ionic cross-links between COO^- and NH_3^+ and the PAA polyelectrolytes in the

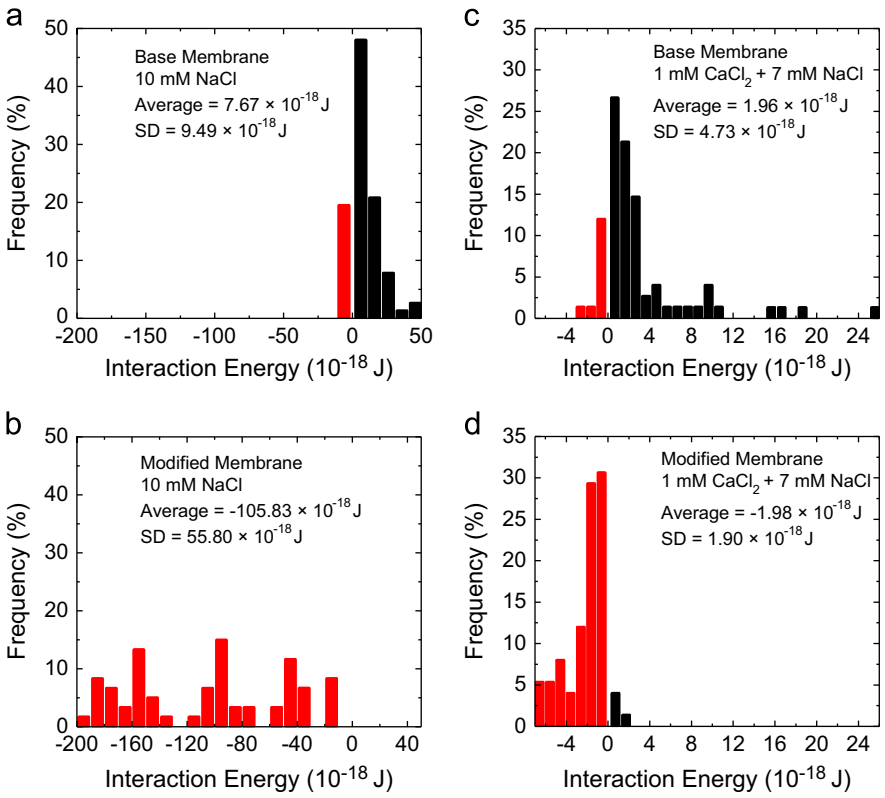

Fig. 9. Work of adhesion distributions for (a) base membrane at 10 mM NaCl, (b) PEM-modified membrane at 10 mM NaCl, (c) base membrane at 1 mM $CaCl_2$+7 mM NaCl, and (d) PEM-modified membrane at 1 mM $CaCl_2$+7 mM NaCl. All measurements were conducted at pH 7.0. Red and black bars represent repulsive (negative) and attractive (positive) interactions between CML colloid probe and membrane surface. (For interpretation of the references to color in this figure legend, the reader is referred to the web version of this article.)

PEM take a loopy conformation [16]. When the PEM is subsequently exposed to a higher pH of 7.0, the COOH groups of PAA become fully deprotonated to form COO^- groups. The unpaired COO^- groups then repel each other due to electrostatic repulsion, leading to the PAA polyelectrolytes in the PEM to take an extended conformation. This change in PAA conformation causes the PEM to undergo considerable swelling and become highly hydrated [16]. The approach of a bacterium into a PEM-modified membrane will result in the compression of the swollen PEM film and removal of some water molecules from the PEM. The compressed PEM will exert an elastic repulsive force on the bacterium due to osmotic stresses and push the bacterium away from the underlying PSU membrane, hence preventing the bacterium from being held to the PSU membrane by strong, short-ranged van der Waals attraction [27,36]. Because the hydrated PEM is highly hydrophilic [16], the bacterium will not adhere to the PEM and can be easily removed from the PEM upon rinsing during the release stages. In the case of a PSU base membrane, no barrier exists to prevent the bacterium from coming into direct contact with the membrane surface, and the bacterium can be held on the membrane surface by strong van der Waals forces that do not allow it to be released when rinsed with the rinsing solutions.

Representative retraction force–separation curves obtained at 1 mM $CaCl_2$+7 mM NaCl for the base and PEM-modified membranes are presented in Fig. 8b. In the case of the base membrane, the CML colloid probe experienced a maximum adhesive force of −0.19 nN upon retraction from the membrane surface. In comparison, similar to the observation at 10 mM NaCl (Fig. 8a), the CML colloid probe experienced a repulsive force when it was pulled off from the PEM-modified membrane surface. However, it is noted that this repulsive force was smaller in magnitude and not as long-ranged as the repulsive force at 10 mM NaCl.

3.6. *Influence of calcium on anti-adhesive properties of PEM-modified membranes*

In order to quantify the propensity of the CML colloid probe to adhere to the base and PEM-modified membranes, the work of adhesion was calculated from each of the retraction force–separation curves. The work of adhesion is defined as the work required to pull the CML colloid probe away from the membrane surface after contact [38,39], and is obtained by integrating the total area under the retract force profiles, as illustrated in Fig. 8b. This work is positive when the force between CML colloid probe and membrane surface is attractive and is negative when the force between the probe and membrane surface is repulsive.

The distributions of the work of adhesion for the base and PEM-modified membranes obtained at 10 mM NaCl are presented in Fig. 9a and b, respectively. For the base membranes, attractive interactions between the CML colloid probe and membrane surface were detected for 80% of the pull-off events. For the PEM-modified membranes, in contrast, repulsive interactions were detected for 100% of the pull-off events. These results showed that the colloid–PEM-modified membrane interactions were strongly repulsive (average work$=-105.83\times10^{-18}$ J) while the colloid–base membrane interactions were slightly adhesive (average work$=7.67\times10^{-18}$ J). The PEM is highly hydrated and swollen at 10 mM NaCl and exerts a strong elastic repulsive force on the colloidal probe which prevents it from adhering to the underlying PSU membrane.

The distributions of the work of adhesion for the base and PEM-modified membranes obtained in the presence of calcium are shown in Fig. 9c and d, respectively. For the base membranes, adhesive interactions between the CML colloid probe and membrane surface were detected for 85% of the pull-off events. Conversely, for the PEM-modified membranes, repulsive

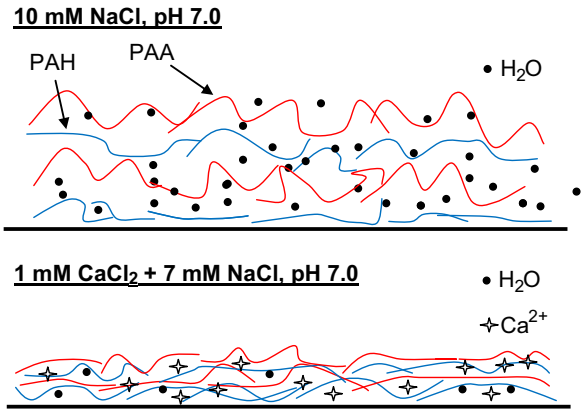

Fig. 10. The PAH/PAA multilayer is highly hydrated and swollen in the absence of calcium (top). In the presence of calcium, the PAH/PAA multilayer becomes less hydrated and less swollen (bottom). The schematics are not drawn to scale and are for illustrative purposes only.

interactions were observed for 93% of the pull-off events. These results indicated that, analogous to the findings at 10 mM NaCl, the colloid–base membrane interactions were generally adhesive (mean work$=1.96\times10^{-18}$ J) while the colloid–PEM-modified membrane interactions were largely repulsive (mean work$=-1.98\times10^{-18}$ J) in the presence of calcium. The less favorable interactions between the colloids and PEM-modified membranes corroborated with the observations that the bacterial deposition on PEM-modified membranes was slower than on base membranes and that the degree of bacterial release after deposition was considerably higher for the PEM-modified membranes.

It is noted that, while the interaction forces between the CML colloid probe and PEM-modified membranes were generally repulsive for both solution chemistries, the repulsive interaction at 10 mM NaCl (average work$=-105.83\times10^{-18}$ J) was significantly stronger than that at 1 mM $CaCl_2$+7 mM NaCl (average work$=-1.98\times10^{-18}$ J). This result is consistent with the noticeably lower removal efficiencies after deposition in the presence of calcium (59% and 68% in Stages 1 and 2, respectively, in Fig. 7b) compared to the removal efficiencies after deposition in the absence of calcium (97% and 99% in Stages 1 and 2, respectively, in Fig. 7a). When a PEM-modified membrane is exposed to calcium, the calcium ions can form complexes with the carboxyl groups of the PAA [40–42] that are within and on the outer surface of the PEM film and thus neutralize the charges of the PAA. Furthermore, calcium can form intermolecular and intramolecular bridges through the formation of calcium complexes with the PAA carboxyl groups [40–42]. Therefore, the PAA polyelectrolytes take a more compact conformation, resulting in the PEM to become less swollen and less hydrated, as illustrated in Fig. 10. Even when the PEM-modified membrane was rinsed with a 1 mM NaCl solution in the second release stage, some residual calcium ions are likely to remain bound to the carboxyl groups of PAA, hence preventing the PEM to return to its fully hydrated state. Therefore, the repulsive force exerted by the less swollen/hydrated PEMs in the presence of calcium are not as strong and long-ranged as the forces exerted by the fully hydrated PEMs in the absence of calcium. Nevertheless, despite the effects of calcium, the PEM modification of membranes can considerably enhance the reversibility of bacterial attachment from ca. 2% to 68% (Fig. 7b).

4. Conclusion

The anti-adhesive properties of PSU membranes that were modified with PEMs comprised of PAH and PAA were investigated in this study. PEMs were assembled on the PSU membranes using the LbL adsorption technique with the employment of a flow cell. XPS analysis of PSU membranes modified with varying number of bilayers demonstrated that the carboxylic acid and nitrogen concentrations increased with increasing bilayers, thus confirming that PAH/PAA PEMs can be successfully assembled on PSU membranes through the LbL technique. The anti-adhesive properties of PEM-modified membranes were evaluated by measuring the deposition kinetics of *E. coli* cells in two solution chemistries (10 mM NaCl and 1 mM $CaCl_2$+7 mM NaCl) and testing the reversibility of bacterial deposition using a direct microscopic observation membrane filtration system. Our results show that the modification of PSU membranes with PEMs can reduce bacterial deposition kinetics by about half both in the absence and presence of calcium. Furthermore, the removal efficiencies were significantly increased after PEM-modification from $<10\%$ to 99% and 68% for bacterial deposition in the absence and presence of calcium, respectively. AFM interaction force measurements showed that the adhesive forces between the CML colloid probe and membrane surfaces were significantly reduced (eliminated in the absence of calcium) after PEM modification. Instead, strong, long-ranged repulsive forces observed between the colloid probe and PEM-modified surfaces inhibited the irreversible attachment of *E. coli* cells on the membrane surfaces. The remarkable bacterial anti-adhesive properties of the PEM-modified membranes were attributed to the highly swollen and hydrated structure of the PEMs which prevent bacteria from being held to the underlying PSU membranes by strong, short-ranged van der Waals attraction. Although the complex formation between the carboxyl groups of the PAAs and calcium resulted in the PEMs to become less hydrated, repulsive interactions between the CML colloid probe and PEM-modified membranes were still dominant in the presence of calcium. In summary, this study demonstrated that PSU membranes modified with PAH/PAA PEMs showed significantly improved bacterial anti-adhesive properties compared to PSU base membranes. Further investigation is required to examine the influence of PEM composition, number of bilayers, and solution chemistries employed for PEM assembly on the anti-adhesive properties of PEM-modified membranes.

Acknowledgments

This work was supported by the National Science Foundation (CBET-1133559) and the Global Water Program at Johns Hopkins University (JHU). L.T. acknowledges funding support from the Dean Robert H. Roy fellowship. We thank Dr. Menachem Elimelech from Yale University for providing us the *E. coli* K12 MG 1655 strain. We acknowledge the assistance from Hyun Sik Choi and Tiffany Wei from the Department of Geography and Environmental Engineering (JHU) with the deposition experiments. The SEM images of the membranes are taken by Dr. Michael McCaffery from the Integrated Imaging Center, Department of Biology (JHU).

Appendix A. Supporting information

Supplementary data associated with this article can be found in the online version at http://dx.doi.org/10.1016/j.memsci.2013.06.031.

References

[1] H. Huang, K. Schwab, J.G. Jacangelo, Pretreatment for low pressure membranes in water treatment: a review, Environ. Sci. Technol. 43 (2009) 3011–3019.

[2] S.T. Kang, A. Subramani, E.M.V. Hoek, M.A. Deshusses, M.R. Matsumoto, Direct observation of biofouling in cross-flow microfiltration: mechanisms of deposition and release, J. Membr. Sci. 244 (2004) 151–165.
[3] M. Pasmore, P. Todd, S. Smith, D. Baker, J. Silverstein, D. Coons, C.N. Bowman, Effects of ultrafiltration membrane surface properties on *Pseudomonas aeruginosa* biofilm initiation for the purpose of reducing biofouling, J. Membr. Sci. 194 (2001) 15–32.
[4] J.S. Baker, L.Y. Dudley, Biofouling in membrane systems – a review, Desalination 118 (1998) 81–89.
[5] C.X. Liu, D.R. Zhang, Y. He, X.S. Zhao, R.B. Bai, Modification of membrane surface for anti-biofouling performance: effect of anti-adhesion and anti-bacteria approaches, J. Membr. Sci. 346 (2010) 121–130.
[6] K. Zodrow, L. Brunet, S. Mahendra, D. Li, A. Zhang, Q.L. Li, P.J.J. Alvarez, Polysulfone ultrafiltration membranes impregnated with silver nanoparticles show improved biofouling resistance and virus removal, Water Res. 43 (2009) 715–723.
[7] S.H. Kim, S.Y. Kwak, B.H. Sohn, T.H. Park, Design of TiO_2 nanoparticle self-assembled aromatic polyamide thin-film-composite (TFC) membrane as an approach to solve biofouling problem, J. Membr. Sci. 211 (2003) 157–165.
[8] M. Herzberg, M. Elimelech, Biofouling of reverse osmosis membranes: role of biofilm-enhanced osmotic pressure, J. Membr. Sci. 295 (2007) 11–20.
[9] S. Kang, E.M.V. Hoek, H. Choi, H. Shin, Effect of membrane surface properties during the fast evaluation of cell attachment, Sep. Sci. Technol. 41 (2006) 1475–1487.
[10] A. Subramani, E.M.V. Hoek, Direct observation of initial microbial deposition onto reverse osmosis and nanofiltration membranes, J. Membr. Sci. 319 (2008) 111–125.
[11] G. Decher, J.D. Hong, Buildup of ultrathin multilayer films by a self-assembly process. 2. Consecutive adsorption of anionic and cationic bipolar amphiphiles and polyelectrolytes on charged surfaces, Ber. Bunsen-Ges. Phys. Chem. 95 (1991) 1430–1434.
[12] G. Decher, J.D. Hong, J. Schmitt, Buildup of ultrathin multilayer films by a self-assembly process. 3. Consecutively alternating adsorption of anionic and cationic polyelectrolytes on charged surfaces, Thin Solid Films 210 (1992) 831–835.
[13] G. Decher, Fuzzy nanoassemblies: toward layered polymeric multicomposites, Science 277 (1997) 1232–1237.
[14] J.W. Ostrander, A.A. Mamedov, N.A. Kotov, Two modes of linear layer-by-layer growth of nanoparticle-polylectrolyte multilayers and different interactions in the layer-by-layer deposition, J. Am. Chem. Soc. 123 (2001) 1101–1110.
[15] J.A. Lichter, K.J. Van Vliet, M.F. Rubner, Design of antibacterial surfaces and interfaces: polyelectrolyte multilayers as a multifunctional platform, Macromolecules 42 (2009) 8573–8586.
[16] J.D. Mendelsohn, S.Y. Yang, J. Hiller, A.I. Hochbaum, M.F. Rubner, Rational design of cytophilic and cytophobic polyelectrolyte multilayer thin films, Biomacromolecules 4 (2003) 96–106.
[17] R. Malaisamy, M.L. Bruening, High-flux nanofiltration membranes prepared by adsorption of multilayer polyelectrolyte membranes on polymeric supports, Langmuir 21 (2005) 10587–10592.
[18] G.Q. Liu, D.M. Dotzauer, M.L. Bruening, Ion-exchange membranes prepared using layer-by-layer polyelectrolyte deposition, J. Membr. Sci. 354 (2010) 198–205.
[19] W.Q. Jin, A. Toutianoush, B. Tieke, Use of polyelectrolyte layer-by-layer assemblies as nanofiltration and reverse osmosis membranes, Langmuir 19 (2003) 2550–2553.
[20] J.W. Wang, Y.X. Yao, Z.R. YueJ. Economy, Preparation of polyelectrolyte multilayer films consisting of sulfonated poly (ether ether ketone) alternating with selected anionic layers, J. Membr. Sci. 337 (2009) 200–207.
[21] R.H. Lajimi, E. Ferjani, M.S. Roudesli, A. Deratani, Effect of LbL surface modification on characteristics and performances of cellulose acetate nanofiltration membranes, Desalination 266 (2011) 78–86.
[22] W. Shan, P. Bacchin, P. Aimar, M.L. Bruening, V.V. Tarabara, Polyelectrolyte multilayer films as backflushable nanofiltration membranes with tunable hydrophilicity and surface charge, J. Membr. Sci. 349 (2010) 268–278.
[23] F. Diagne, R. Malaisamy, V. Boddie, R.D. Holbrook, B. Eribo, K.L. Jones, Polyelectrolyte and silver nanoparticle modification of microfiltration membranes to mitigate organic and bacterial fouling, Environ. Sci. Technol. 46 (2012) 4025–4033.
[24] S.R. Qi, C.Q. Qiu, Y. Zhao, C.Y.Y. Tang, Double-skinned forward osmosis membranes based on layer-by-layer assembly-FO performance and fouling behavior, J. Membr. Sci. 405 (2012) 20–29.
[25] J. Kochan, M. Scheidle, J. van Erkel, M. Bikel, J. Buchs, J.E. Wong, T. Melin, M. Wessling, Characterization of antibacterial polyethersulfone membranes using the respiration activity monitoring system (RAMOS), Water Res. 46 (2012) 5401–5409.
[26] A. Adout, S. Kang, A. Asatekin, A.M. Mayes, M. Elimelech, Ultrafiltration membranes incorporating amphiphilic comb copolymer additives prevent irreversible adhesion of bacteria, Environ. Sci. Technol. 44 (2010) 2406–2411.
[27] M. Elimelech, J. Gregory, X. Jia, R.A. Williams, Particle Deposition and Aggregation: Measurement, Modelling and Simulation, Butterworth-Heinemann, Oxford, England, 1995.
[28] Q.L. Li, M. Elimelech, Organic fouling and chemical cleaning of nanofiltration membranes: measurements and mechanisms, Environ. Sci. Technol. 38 (2004) 4683–4693.
[29] S. Kang, A. Asatekin, A.M. Mayes, M. Elimelech, Protein antifouling mechanisms of PAN UF membranes incorporating PAN-g-PEO additive, J. Membr. Sci. 296 (2007) 42–50.
[30] B.X. Mi, M. Elimelech, Organic fouling of forward osmosis membranes: fouling reversibility and cleaning without chemical reagents, J. Membr. Sci. 348 (2010) 337–345.
[31] J.A. Brant, A.E. Childress, Colloidal adhesion to hydrophilic membrane surfaces, J. Membr. Sci. 241 (2004) 235–248.
[32] S. Lee, M. Elimelech, Relating organic fouling of reverse osmosis membranes to intermolecular adhesion forces, Environ. Sci. Technol. 40 (2006) 980–987.
[33] H.N. Kim, S.L. Walker, Escherichia coli transport in porous media: influence of cell strain, solution chemistry, and temperature, Colloid Surf. B 71 (2009) 160–167.
[34] S. Kang, M. Elimelech, Bioinspired single bacterial cell force spectroscopy, Langmuir 25 (2009) 9656–9659.
[35] T.L. Byrd, J.Y. Walz, Interaction force profiles between *Cryptosporidium parvum* oocysts and silica surfaces, Environ. Sci. Technol. 39 (2005) 9574–9582.
[36] J. Israelachvili, Intermolecular and Surface Forces, Academic Press, London, England, 1991.
[37] J.A. Lichter, M.T. Thompson, M. Delga-Dillo, T. Nishikawa, M.F. Rubner, K.J. Van Vliet, Substrata mechanical stiffness can regulate adhesion of viable bacteria, Biomacromolecules 9 (2008) 1571–1578.
[38] R. Pericet-Camara, G. Papastavrou, S.H. Behrens, C.A. Helm, M. Borkovec, Interaction forces and molecular adhesion between pre-adsorbed poly(ethylene imine) layers, J. Colloid Interface Sci. 296 (2006) 496–506.
[39] K.L. Chen, S.E. Mylon, M. Elimelech, Enhanced aggregation of alginate-coated iron oxide (hematite) nanoparticles in the presence of calcium, strontium, and barium cations, Langmuir 23 (2007) 5920–5928.
[40] L. Dupont, A. Foissy, R. Mercier, B. Mottet, Effect of calcium-ions on the adsorption of polyacrylic-acid onto alumina, J. Colloid Interface Sci. 161 (1993) 455–464.
[41] B. Kriwet, T. Kissel, Interactions between bioadhesive poly(acrylic acid) and calcium ions, Int. J. Pharm. 127 (1996) 135–145.
[42] R. Schweins, K. Huber, Collapse of sodium polyacrylate chains in calcium salt solutions, Eur. Phys. J. E 5 (2001) 117–126.